Atomic-structure changes of 30° partial-dislocation cores due to excess carriers in GaP

Sena Hoshino,[1] Shuji Oi,[1] Yu Ogura,[1] Tatsuya Yokoi,[1] Yan Li,[2] Atsutomo Nakamura,[2,3] and Katsuyuki Matsunaga[1,4,*]

[1]*Department of Materials Physics, Nagoya University, Furo-cho, Chikusa, Nagoya 464–8603, Japan*

[2]*Department of Mechanical Science and Bioengineering, Osaka University, 1–3 Machikaneyama-cho, Toyonaka 560–8531, Japan*

[3]*Presto, Japan Science and Technology Agency (JST), 4-1-8, Honcho, Kawaguchi-shi, Saitama 332-0012, Japan*

[4]*Nanostructures Research Laboratory, Japan Fine Ceramics Center, 2-4-1 Mutsuno, Atsuta, Nagoya 456–8587, Japan*

(Received 31 January 2024; accepted 12 August 2024; published 12 September 2024)

It was experimentally reported that light illumination leads to reduced deformation stresses in some III-V compound semiconductors such as GaP. This phenomenon is known as the negative photoplastic effect, which is expected to originate from interactions between photoexcited carriers and glide dislocations. To clarify its physical origin at the atomic and electronic levels, density-functional-theory calculations were performed for Shockley 30° partial dislocations in GaP. In the absence of excess carriers, both Ga and P cores of the partial dislocations were found to have reconstructed structures that are energetically most stable. This can be understood by the fact that dangling-bond-like states at undercoordinated atoms of the dislocation cores are removed by core reconstruction. In the presence of excess carriers that would be formed by light illumination, the reconstructed Ga and P cores were able to trap excess holes and electrons, respectively, and were subsequently transformed to unreconstructed structures. It was also found that the unreconstructed structures due to excess carriers tend to have smaller potential barrier heights for dislocation glide, as compared to the pristine reconstructed structures without any excess carriers. This is in good agreement with the increased dislocation mobility in GaP under external light illumination that has been experimentally reported.

DOI: 10.1103/PhysRevMaterials.8.093605

I. INTRODUCTION

III-V group inorganic compound semiconductors have received a lot of attention due to their excellent optical and electronic properties, having many applications such as light-emitting diodes, laser diodes, and photovoltaic cells [1]. This class of materials, however, are in general brittle and easily fracture at room temperature [2], leading to their limited processability and reliability. In this regard, light illumination has been reported to alter plasticity or hardness of inorganic compound semiconductors. This phenomenon is called the photoplastic effect (PPE) and is classified into negative PPE (n-PPE) and positive PPE (p-PPE). The n-PPE corresponding to decreased flow stresses or hardnesses under external light illumination was observed for some III-V group compound semiconductors of GaAs and GaP [3–5]. On the other hand, II-VI group semiconductors such as ZnS and CdS were found to exhibit the p-PPE where external light illumination increases flow stresses [6–14]. Since plastic deformation is mediated by dislocation glide, it is most likely that external light illumination can strongly affect dislocation mobility.

When a semiconducting material is irradiated by light with an energy higher than its band gap, electron-hole pairs are generated via band-to-band transition. The PPE is thus thought to arise from interactions between such excited carriers and glide dislocations. In this regard, our recent theoretical calculations showed favorable core structures of glide dislocations with and without excess carriers in II-VI group compound semiconductors [15–18]. It was found that in the absence of excess carriers, the glide partial dislocations have unreconstructed structures with undercoordinated atoms at the cores. In the presence of excess carriers, however, the partial-dislocation cores were found to trap excess carriers by their excess electrostatic potentials and further undergo atomic reconstruction by the formation of like-atom bonds at the cores. From these results, a plausible mechanism of the p-PPE is that light illumination reduces potential energies of glide partial dislocations by such core reconstruction and in turn increases Peierls potential barriers for dislocation glide (decreased dislocation mobility), leading to increased flow stresses. In fact, reduced dislocation mobility in ZnS under light illumination was also confirmed experimentally by creep mechanical tests at room temperature [19].

In contrast, it remains unknown whether such a mechanism of atomic-structure change of the dislocation cores due to excess carriers proposed for II-VI group semiconductors can be applied to III-V group semiconductors. Unlike II-VI group semiconductors, for instance, GaAs showed reduced deformation stresses by light illumination (n-PPE), which was ascribed to increased dislocation mobility during light illumination [3–4]. Increased dislocation mobility by external light was also observed in GaP [5]. To account for such increased dislocation mobility in GaAs and GaP [3–5], the recombination-enhanced dislocation glide (REDG) mechanism [20–22] seems to be sometimes used, where excess carriers generated by light illumination recombine nonradiatively at dislocation cores, simultaneously emitting phonons

*Contact author: kmatsunaga@nagoya-u.jp

TABLE I. Calculated band-gap energies (E_g) obtained from GGA, GGA+U, and HSE calculations with the experimental data.

		GGA+U: $U = -10$ eV on P-3p			
	GGA_PBE	Previous work[a]	This work	HSE06 $\alpha = 0.2$	Experiment[b]
E_g (eV)	1.65	2.22	2.14	2.22	2.26

[a]Reference [29].
[b]Reference [32].

that accelerate dislocation glide. However, this mechanism was originally put forward to account for light-emitting degradation of the semiconductors due to anomalous dislocation generation during operation, and thus was not intended for plastic deformation behavior of the n-PPE.

In the present study, density-functional-theory (DFT) calculations were performed to investigate dislocation core structures with and without excess carriers in GaP, which is a typical III-V group compound semiconductor. Dislocation formation energies were evaluated to clarify the stability of the core structures with and without excess carriers. Local densities of states (LDOSs) of the dislocation cores were analyzed to investigate specific electronic structures due to the dislocation cores. In addition to the generalized-gradient approximation with Hubbard U correction (GGA+U) calculations, hybrid functional calculations were also performed to check the validity of the results obtained by GGA+U calculations. A physical origin of the increased dislocation mobility in GaP under light illumination was clarified in terms of atomic-structure change and energetics of the dislocation cores.

II. COMPUTATIONAL METHOD

A. DFT calculations

DFT calculations were performed using the projector augmented wave (PAW) method implemented in the Vienna *ab initio* Simulation Package (VASP) [23,24]. The exchange-correlation energy was computed using the generalized-gradient approximation (GGA) with the Perdew-Burke-Ernzerhof (PBE) formalism [25]. A plane-wave cutoff energy was set to 450 eV for all cases. The 3d, 4s, and 4p orbitals for Ga and the 3s and 3p orbitals for P were treated as valence electrons in the PAW potentials. GGA calculations typically underestimate the band-gap energy, which often affects defect formation energies [26,27]. To reproduce the experimental band gap, GGA+U calculations [28] were thus performed by setting an effective U parameter to –10 eV for the P-3p orbitals [29].

To check the validity of GGA+U calculations with the negative U value, standard GGA-PBE calculations with smaller supercells involving a partial dislocation pair as described below (144-atom supercells for unreconstructed dislocation cores and 288-atom ones for reconstructed dislocation cores) were performed. From comparisons of dislocation formation energies between GGA+U and GGA (see Fig. S1 in the Supplemental Material [30]), it was confirmed that absolute values of the formation energies are somewhat dependent on whether GGA+U or GGA is used, but the overall trend in the relative stability of neutral and charged partial dislocations over the entire Fermi energy range is not affected by the DFT approaches.

For a further cross-check of the calculated results, Heyd-Scuseria-Ernzerhof (HSE [31]) hybrid functional calculations were also performed by setting the amount of exact exchange α to 20%. Table I indicates that band-gap energies of zinc-blende structured GaP perfect crystal (E_g) obtained by the GGA+U and HSE calculations are close to the experimental value [32].

As will be described later, dislocation cores were modeled mainly with parallelepiped-shaped supercells containing 288 atoms [15]. Here, the x- and z-axes were parallel to the $[11\bar{2}]$ and $[\bar{1}10]$ directions of the cubic zinc-blende structure, respectively. For the k-space sampling, a $1 \times 2 \times 6$ grid was used. For structural optimization, the energy and force convergence criteria were set to 10^{-6} eV and 10^{-2} eV/Å, respectively. For HSE calculations, 144-atom supercells were used with a $1 \times 2 \times 6$ k-mesh grid. In this case, single-point calculations were performed using the dislocation-containing supercells relaxed by GGA+U calculations.

B. Dislocation modeling

GaP with the zinc-blende structure has a primary slip system $\{111\}\langle 1\bar{1}0\rangle$. Previous experimental observations by weak-beam electron microscopy indicated the presence of 30°-30° Shockley partial dislocation pairs separated by a {111} stacking fault in GaP [33]. Therefore, such Shockley 30° partial dislocations with a Burgers vector of $1/6\langle\bar{2}11\rangle$ were focused as typical glide dislocations in GaP. Since the {111} plane is polar, the partial dislocation cores are off-stoichiometric and hence are either Ga-rich or P-rich, which are hereafter referred to as the Ga core and the P core, respectively. The 288-atom supercell contains a Ga core and a P core separated by a {111} stacking fault with its width (d_{SF}) of 2.6 nm in order to satisfy three-dimensional periodic boundary conditions and overall stoichiometry. Here the dislocation lines were set to be parallel to the z-axis ($[\bar{1}10]$). The dislocation cores were located at the quadrupole positions over periodic supercell images to cancel elastic interactions between dislocations at the cores even in the finite-sized supercells [34].

For both the Ga and P cores, unreconstructed and reconstructed structures were considered as initial structures and were relaxed by structural optimization. The initial unreconstructed structures were obtained by displacing atoms according to the elastic theory, as shown in Figs. 1(a) and 1(b). However, these structures have undercoordinated atoms along the dislocation lines. In this case, it is likely that the

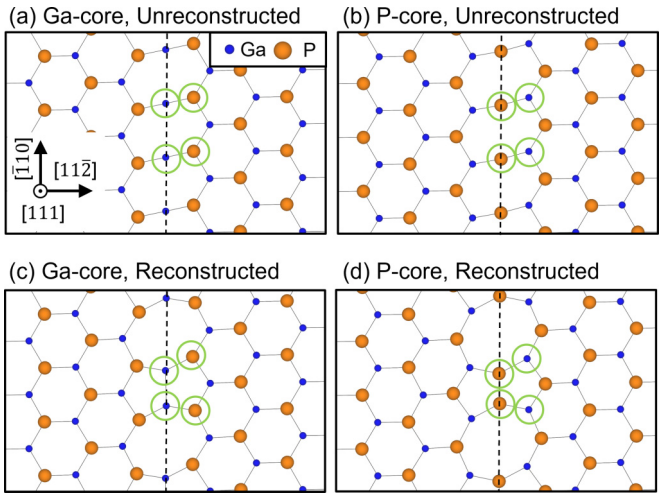

FIG. 1. Calculated atomic structures at the Ga and P cores of the 30° partial dislocations in the neutral charge state ($q = 0$). The blue and orange balls represent Ga and P atoms, respectively, and the dashed lines represent the dislocation lines. Atoms circled in green are used for LDOS analyses in Fig. 2.

unreconstructed structures change to reconstructed ones so as to eliminate dangling bonds of the undercoordinated atoms, as indicated by previous studies [35–42]. For the 30° partials, double period (DP) structures of reconstructed dislocation cores were reported, in which undercoordinated like atoms form new bonds along the dislocation lines [Figs. 1(c) and 1(d)]. Such a DP structure was also considered in the present study. Since the DP structure has doubled periodicity of the unreconstructed structure along the z axis, the number of atoms in the supercells for the DP reconstructed structures was 576.

Our recent study for II-VI compound semiconductors [16] showed that energetic positions of defect-induced levels due to dislocations within the band gaps can vary with supercell size. To examine such a supercell-sized dependence in GaP, LDOS curves of the unreconstructed 30° partial pairs were plotted against d_{SF} in Fig. 2: $d_{SF} = 1.3$, 2.0, 2.6, and 3.3 nm correspond to the supercells of 48, 144, 288, and 480 atoms, respectively. It was found that the shapes and positions of the defect-induced levels are almost the same regardless of the supercell sizes over 288 (576) atoms ($d_{SF} \geqslant 2.6$ nm). Although experimental d_{SF} was around 4–8 nm [33], it is reasonable to consider that the fundamental characteristics of electronic structures at the dislocation cores can be well described even by the 288-atom (576-atom) supercells with $d_{SF} = 2.6$ nm. Therefore, the results mainly shown below are the ones from the 288-atom (the unreconstructed structure) and the 576-atom (the reconstructed structure) supercells.

C. Dislocation formation energy ΔE_f

To determine energetically stable atomic structures of the Ga and P cores, dislocation formation energies $\Delta E_f(q)$ were calculated by

$$\Delta E_f(q) = E_T(\text{dislocation},\ q) - E_T(\text{perfect}) + q(E_{VBM} + \varepsilon_F). \quad (1)$$

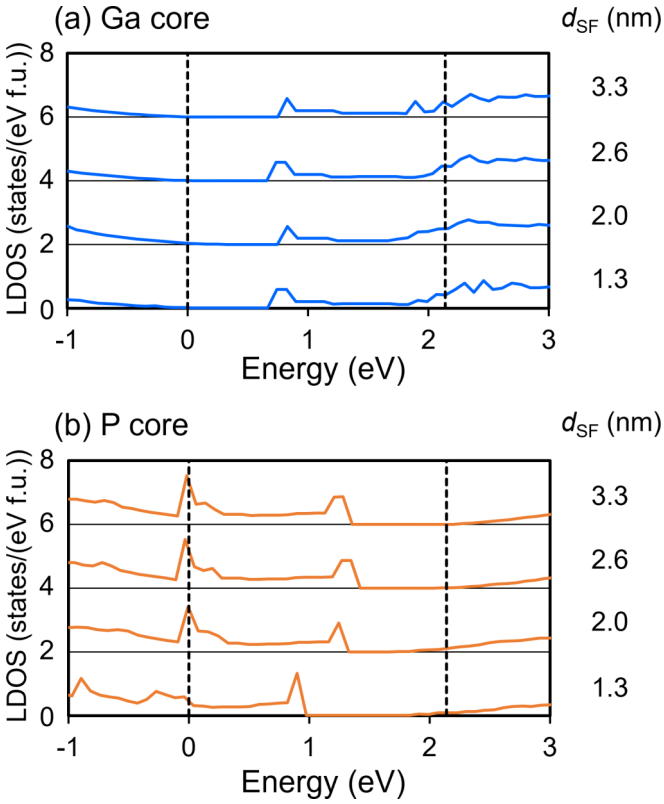

FIG. 2. LDOS curves of (a) the Ga core and (b) the P core of the unreconstructed partial dislocations with different d_{SF} (1.3, 2.0, 2.6, and 3.3 nm), obtained from the GGA+U calculations. The VBM and CBM of the perfect crystal are shown by the vertical dashed lines. These LDOS curves are obtained from the atoms circled in light green in Fig. 1.

E_T(dislocation, q) and E_T(perfect) are the total energies of the 288-atom (or 576-atom) supercells of a dislocation pair and the perfect crystal, respectively. q is a charge of the partial-dislocation pair. To investigate the effects of excess carriers on the dislocation formation energies, excess electrons or holes were independently introduced into the supercells, and the numbers of excess carriers were then changed in the range of q from –4 to +4. For example, if one electron is added to (removed from) the supercell, the q value is equal to –1 (+1). E_{VBM} is the energy of the valence-band maximum (VBM) in the perfect crystal, and ε_F is the Fermi energy measured from the VBM. Since E_{VBM} of the finite-sized supercells with a partial-dislocation pair is different from that of the perfect crystal, E_{VBM} was corrected by average electrostatic potentials as follows:

$$E_{VBM} = E_{VBM}^{\text{perfect}} + V_{ave}^{\text{dislocation}} - V_{ave}^{\text{perfect}}, \quad (2)$$

where E_{VBM}^{perfect} is the VBM energy of the perfect supercell, obtained from an energy difference between E_T(perfect, $q = 0$) and E_T(perfect, $q = +1$). $V_{ave}^{\text{dislocation}}$ and V_{ave}^{perfect} are average electrostatic potentials of atomic sites farthest from the dislocation cores and in the perfect crystal, respectively.

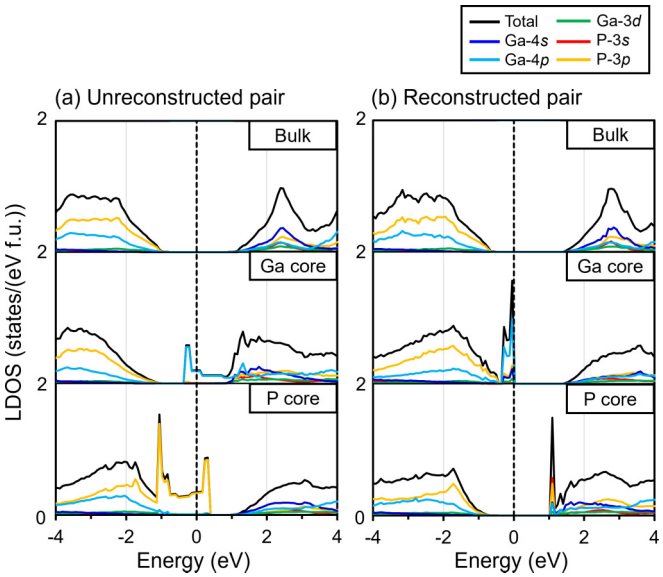

FIG. 3. LDOS curves of (a) the unreconstructed and (b) the reconstructed partial-dislocation pairs with $q = 0$ obtained from GGA+U calculations. The LDOS of the bulk is also shown in the top panel. The vertical dashed lines represent the highest occupied levels.

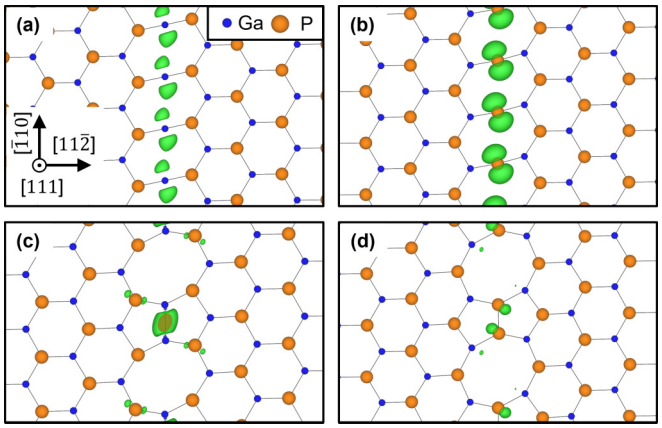

FIG. 4. The band-decomposed charge densities of the defect-induced levels for the unreconstructed (a) Ga core and (b) P core and the reconstructed (c) Ga core and (d) P core with $q = 0$.

III. RESULTS

A. Atomic and electronic structures of the dislocation cores with $q = 0$

This section discusses electronic and atomic structures of the 30° partial dislocation pair in the absence of excess carriers (i.e., $q = 0$). Figures 1(a) and 1(c) show atomic structures of the Ga core after structural optimization. For the unreconstructed structure [Fig. 1(a)], the Ga atoms on the dislocation line are threefold-coordinated by P atoms, and their interatomic distance of Ga-Ga is 0.380 nm. For the reconstructed structure [Fig. 1(c)], these undercoordinated Ga atoms clearly come close to each other, forming Ga-Ga bonds with an interatomic distance of 0.249 nm. Similarly, the unreconstructed P core also has threefold-coordinated P atoms (the P-P distance is 0.380 nm), whereas the reconstructed core has a P-P bond with an interatomic distance of 0.212 nm, as shown in Figs. 1(b) and 1(d).

It was found that when both the Ga and P cores have reconstructed structures in the supercell, which is referred to as the reconstructed pair, $\Delta E_{\rm f}(q = 0)$ is lower by 1.38 eV/nm than that of the unreconstructed pair. Therefore, the 30° partial dislocations in GaP favor the reconstructed structures as the pristine core structures.

To clarify this issue in more detail, their electronic structures were analyzed. Figures 3(a) and 3(b) show LDOS curves of the unreconstructed and reconstructed pairs in the 288-atom and 576-atom supercells, respectively, which are obtained from the atoms circled in green in Fig. 1. The bulk LDOS curve was obtained from LDOSs of the Ga and P atoms furthest from the dislocation cores. For the unreconstructed pair [Fig. 3(a)], the Ga core exhibits broad defect-induced levels below the conduction-band minimum (CBM) in bulk, which are formed mainly by the Ga-4p orbitals, and the P core also exhibits broad defect-induced levels above the VBM in bulk, which mainly consist of P-3p orbitals. Notice that both defect-induced levels are partially occupied, as seen around the vertical dashed line corresponding to the highest electron occupied level. For the reconstructed pair [Fig. 3(b)], the Ga core has the fully occupied extra levels localized just above the VBM, whereas the P core has the unoccupied extra levels localized just below the CBM. These defect levels are dominated by the Ga-4p and P-3sp orbitals at the Ga and P cores, respectively.

Such differences in defect-induced levels within the band-gap area can be understood in terms of dangling bonds having unpaired electrons in covalent semiconductors. As stated above, the Ga (P) core involves the undercoordinated Ga (P) atoms along the dislocation line. When it is assumed that GaP is strongly covalent, the undercoordinated atoms can have dandling bonds, which results in the formation of defect-induced levels with partial electron-occupancy within the band gap. This is the case of Fig. 3(a). Such features of the dangling-bond states at the different cores can also be confirmed from spatial distributions of the defect-induced levels displayed in Figs. 4(a) and 4(b). In contrast, such dangling bonds having unpaired electrons can be favorably removed by the formation of the like-atom pairs of Ga-Ga or P-P. This corresponds to the fully electron-occupied or electron-unoccupied defect-induced levels appearing around VBM and CBM in Fig. 3(b). In the case of the Ga core, the fully electron-occupied levels are formed just above the VBM. Since the defect-induced levels of the reconstructed Ga core are also composed mainly of Ga-4p orbitals, they are referred to as deep donor-like levels. As can be seen in Fig. 4(c), the Ga-4p orbitals are localized and have bonding interactions between the adjacent Ga atoms at the core, so that the energy position can be lowered, even compared with that of the defect-induced levels in the unreconstructed Ga core. At the P core, however, the defect-induced levels composed of P-3sp orbitals should have originally antibonding characters between P atoms, because they come from the valence band. Such a feature of the defect-induced level can be imagined from Fig. 4(d). As a result, atomic reconstruction at the P core can make the defect-induced levels energetically higher.

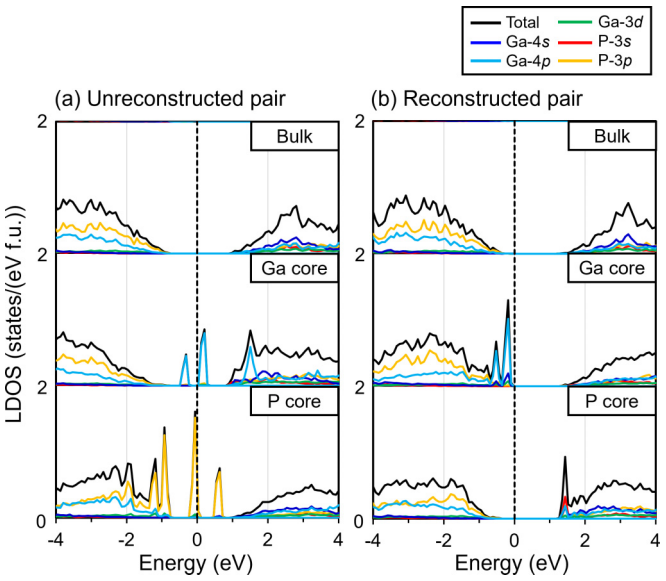

FIG. 5. LDOS curves of (a) the unreconstructed and (b) the reconstructed partial-dislocation pairs with $q = 0$ obtained from HSE calculations. The LDOS of the bulk is also shown in the top panel. The vertical dashed lines represent the highest occupied levels.

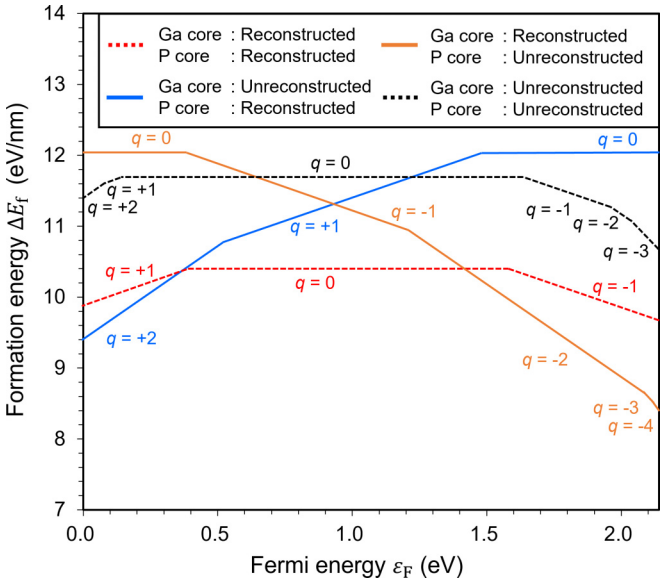

FIG. 6. $\Delta E_{\rm f}$ (q) as a function of $\varepsilon_{\rm F}$ obtained from GGA+U calculations for the 288-atom and 576-atom supercells. Four different types of partial dislocation pairs are considered: the unreconstructed pair, the reconstructed pair, and the pairs of unreconstructed and reconstructed cores.

This corresponds to the fact that holes originally located at the undercoordinated P atoms of the core are energetically more stabilized by such atomic reconstruction.

It is worth mentioning here that the above features of the LDOSs for the unreconstructed and reconstructed cores can also be confirmed from HSE calculations (Fig. 5). In the unreconstructed cores, the defect-induced levels above the VBM and below the CBM appear in a more discrete manner than those of Fig. 3(a). However, they are still partially electron-occupied, and they are composed of the Ga-4p orbitals at the Ga core (donorlike states coming from the CBM) and of the P-3p orbitals at the P core (acceptorlike states coming from the VBM). As a result of atomic reconstruction, these levels are much more localized in their energy positions just above the VBM and below the CBM. This ensures the validity of the LDOS features obtained by the present GGA+U calculations.

B. Dislocation formation energy in the presence of excess carriers

Figure 6 shows calculated $\Delta E_{\rm f}(q)$ values for different q as a function of $\varepsilon_{\rm F}$. As can be seen from Eq. (1), $\Delta E_{\rm f}(q)$ is dependent on q that is a slope of the $\Delta E_{\rm f}(q)$ profile against $\varepsilon_{\rm F}$. In this case, only the lowest $\Delta E_{\rm f}(q)$ value among those with different q values was plotted at respective $\varepsilon_{\rm F}$. The range of $\varepsilon_{\rm F}$ was set to the band-gap energy (E_g) obtained from the GGA+U calculations (see Table I). It is also noted that four types of dislocation pairs were considered here. In the above sections, the unreconstructed and the reconstructed pairs were discussed in the state of $q = 0$. In addition, two more different pairs of the partial dislocations were taken into account: those with a reconstructed Ga core and an unreconstructed P core, and with an unreconstructed Ga core and a reconstructed P core. This is because these dislocation pairs were found to become more stable depending on their charge state q (see the details below).

According to the results in Sec. III A, the electronic structures of the Ga and P cores in the ground state can be schematically illustrated as shown in Fig. 7(a). The deep donor-like levels are fully occupied at the reconstructed Ga core, while the deep acceptor-like levels are fully unoccupied at the reconstructed P core. When it comes to the case of light illumination, electron and hole pairs can be formed by band-to-band transition in GaP. If the excited carriers are produced near the dislocations, it can be expected that formed carriers

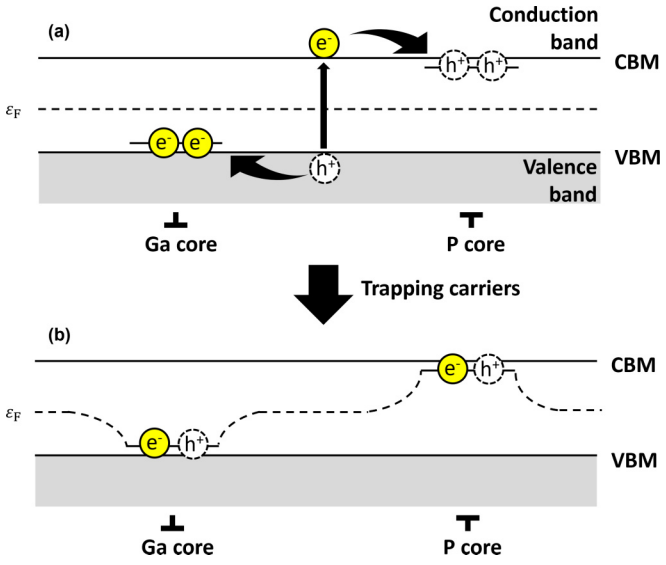

FIG. 7. Schematic band structure of the reconstructed pair (a) before and (b) after trapping carriers.

of an electron and a hole are separated from each other before recombination. Then, the electrons (holes) can be trapped at the deep acceptor-like levels at the P core (the deep donor-like states at the Ga core). This situation is illustrated in Fig. 7(b). This takes place because the deep acceptor-like levels at the P core (the deep donor-like states at the Ga core) are fully unoccupied (occupied). In the normal DFT calculations providing the ground-state electronic structure for a given atomic arrangement, a situation such as that shown in Fig. 7(b) in the presence of an electron-hole pair cannot be realized. In this study, instead, excess electrons and holes were added to the supercells independently, and the most stable atomic structures of the dislocation pairs and their $\Delta E_{\rm f}(q)$ values were calculated.

It can be seen from Fig. 6 that when $\varepsilon_{\rm F}$ is located at $E_g/2$ (the nondoped system), the neutral reconstructed pair is energetically most stable (see also Sec. III A). In the presence of excess electrons ($\varepsilon_{\rm F}$ close to the CBM), the partial dislocation pair with a reconstructed Ga core and an unreconstructed P core has the smallest $\Delta E_{\rm f}(q)$ value in the charge state of $q = -3$ or -4. As shown in Figs. 3(b) and 4(d), excess electrons are trapped at the antibonding defect-induced levels that are composed of P-3sp orbitals at the P core. Then the reconstructed P-P atomic pair is no longer stable, so that the P core is transformed into the unreconstructed structure.

In contrast, the presence of excess holes ($\varepsilon_{\rm F}$ close to the VBM) results in the much smaller $\Delta E_{\rm f}(q)$ value for the partial dislocation pair with an unreconstructed Ga core and a reconstructed P core with $q = +2$. This means that excess holes can make the unreconstructed Ga core more stable. This is also explained from Figs. 3(b) and 4(c). Excess holes can be energetically more favorable by being trapped at the electron-occupied defect-induced levels at the Ga core. The electron-occupied defect levels have a bonding character of the Ga-4p orbitals, so that holes trapped at the defect-induced levels can make the reconstructed Ga-Ga bond less stable. Excess carriers formed by external light can change the atomic structures of the originally reconstructed dislocation cores in GaP.

Charged defects treated in the periodic supercell calculations can be subjected to artificial Coulombic interactions with the neutralizing background charges and their periodic images, and thus supercell-sized effects on defect energetics should be checked to discuss the relative stability of the defects [26,43]. Since the infinite straight dislocations lying along the z direction are treated in the present supercell calculations, only two-dimensional scaling of the supercell size L (normal to the z direction) is meaningful, which leads, however, to a logarithmic divergence of the formation energies [43]. Moreover, dislocations have elastic fields extending over the dislocation cores (radius of r_c), and the elastic dislocation energies are also logarithmic divergent with increasing dislocation radius R as $\sim \mu b^2 \ln(R/r_c)$ (μ is the shear modulus and b is the Burgers vector) [44,45]. It is noted that R is usually taken to be half of a distance between nearest-neighboring dislocations, namely $R \sim L/4$ in the supercells containing a dislocation dipole. Based on these facts, convergence of the formation energies of dislocations cannot be obtained by extrapolation to infinite L. In the present study, therefore, the calculated formation energies of the partial dislocation pairs

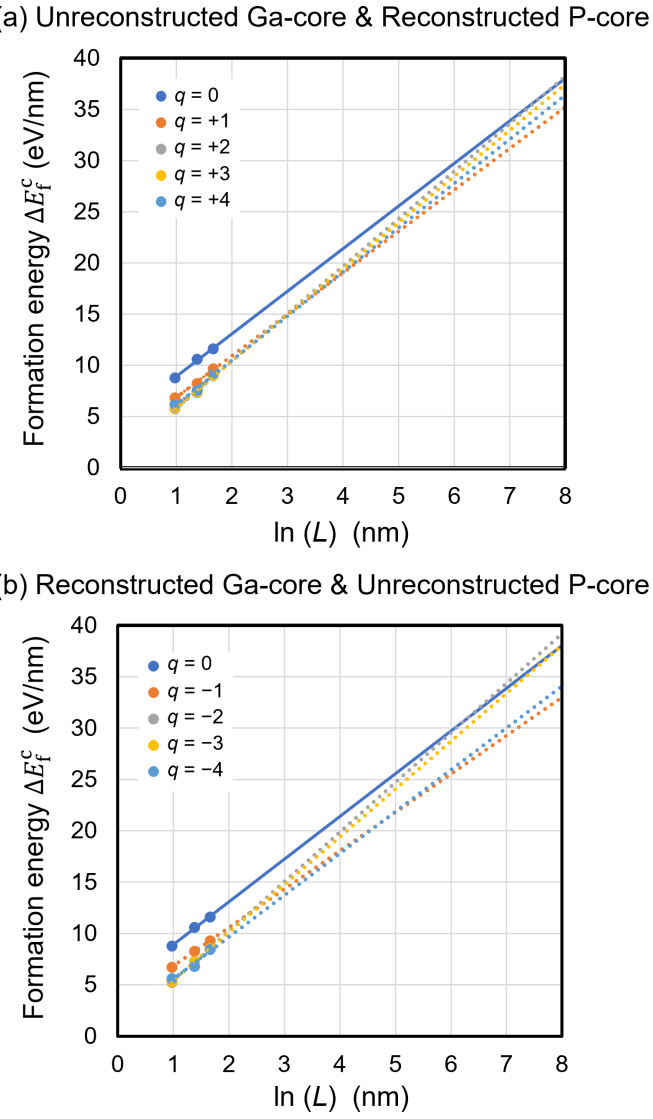

FIG. 8. Supercell-sized dependence of corrected formation energies $\Delta E_{\rm f}^{c}(q)$ of the neutral and charged dislocations. (a) The positively charged Ga core, and (b) the negatively charged P core. Such charged partial-dislocation cores are unreconstructed.

with an unreconstructed Ga core and a reconstructed P core at $\varepsilon_{\rm F}$ = VBM (corresponding to the positively charged Ga cores) and with a reconstructed Ga core and an unreconstructed P core at $\varepsilon_{\rm F}$ = CBM (corresponding to the negatively charged P cores) were plotted against $\ln(L)$, and were linearly fitted and extrapolated to the larger $\ln(L)$ range, as shown in Fig. 8. It should be noted here that the partial dislocation pairs in the supercells sandwich stacking faults with $d_{\rm SF} = L/2$ and thus $\Delta E_{\rm f}(q)$ in Eq. (1) involves the stacking fault energies ($\gamma_{\rm SF}$) that have a linear L dependence. Therefore, $\Delta E_{\rm f}(q)$ was corrected as $\Delta E_{\rm f}^{c}(q) = \Delta E_{\rm f}(q) - \gamma_{\rm SF} A_{\rm SF}$ in this analysis ($A_{\rm SF}$ is the stacking-fault area, and $\gamma_{\rm SF}$ separately calculated is 0.22 eV/nm^2), in order to extract the $\ln(L)$ dependence of $\Delta E_{\rm f}(q)$ of the neutral and charged dislocations.

An average distance between dislocations in the real crystal system was invoked to facilitate the discussion in Fig. 8. In our previous study, for instance, dislocation densities (ρ) in

deformed ZnS were found to be more than $10^8\,\mathrm{cm}^{-2}$ and increase more with increasing plastic deformation [9]. If a similar dislocation density is assumed in GaP, the average distance between dislocations ($= 1/\sqrt{\rho} = L/2$) is less than 10^3 nm, which corresponds to $\ln(L) < 7.6$. From extrapolation of the formation energies to such a $\ln(L)$ range, it was found that the charged states of the unreconstructed Ga and P cores tend to be more stable than their neutral states. This ensures that the partial dislocations in GaP can be charged in the presence of excess electrons and holes that would be excited by external light.

It is also noted that the charged unreconstructed P core has a slightly different atomic structure from the neutral one. Figure S2 in the Supplemental Material shows the reconstructed Ga core and the unreconstructed P core with $q = -4$ [30]. In the charged and unreconstructed P core, the bond angle of the Ga-P-Ga bonds located at the center of the core becomes narrower from 129.6° in the charge neutral state [Fig. 1(b)] to 121.1° [Fig. S2(b) in the Supplemental Material [30]]. In this case, dangling-bond states at the undercoordinated P atoms at the core involve more electrons than those in the charge neutral state, which may affect the bond angle at the dislocation core.

IV. DISCUSSION

As shown above, the partial dislocation cores in GaP are subjected to their atomic-structure changes from the reconstructed structures to the unreconstructed ones in the presence of excess carriers. Such atomic-structure changes at the cores may affect their dislocation mobilities. In a thermal activation process, a dislocation velocity υ in the kink-pair mechanism can be expressed as [46,47]

$$\upsilon = \upsilon_0 \exp\left(-\frac{\Delta H}{kT}\right). \tag{3}$$

In Eq. (3), υ_0 corresponds to a preexponential factor related to the geometry of the kink pair, k is the Boltzmann constant, and T is a temperature. ΔH indicates an enthalpy of the kink-pair formation, and it is also described as $\Delta H = \Delta E + \Delta P - W$, where ΔE is the elastic energy, ΔP is the Peierls energy, and W is the work done by an applied stress. ΔE is proportional to μb^2, and thus it is independent of the dislocation core structure itself. In contrast, when a rectangular kink shape is assumed for instance, ΔP depends on the shape and height of the Peierls-potential barrier [47]. In particular, the Peierls-potential barrier height is responsible for migration of the kink pair, which strongly affects the dislocation velocity.

In the present study, therefore, evaluation of Peierls-potential barriers for dislocation glide was attempted. To address this issue initially, glide motion of the Ga-core dislocations in the neutral and charged states ($q = +4$) was investigated by nudged elastic band (NEB) calculations [48]. In the present NEB calculations, specific intermediate atomic structures of the dislocation cores around the saddle points of their Peierls potentials, reported by Huang *et al.* [49], were used as the central image. Some more images between the initial (or final) structure and the central intermediate structure (see Fig. 9) were taken to investigate the potential profiles. It can be seen in Fig. 9 that the Ga core with $q = 0$ forms Ga-Ga bonds along the dislocation line even in the intermediate structure [Fig. 9(a)], but this is not the case with the Ga core with $q = +4$ [Fig. 9(c)]. It is also noted that the stacking-fault widths between the partial dislocations in the supercells are also varied during the dislocation glide. On the basis of the stacking-fault energy γ_{SF} of $0.22\,\mathrm{eV/nm}^2$ separately calculated, therefore, correction of total-energy changes due to the stacking fault widths was also made to obtain the Peierls potentials. During the NEB calculations, the atomic structure of the reconstructed P core was fixed.

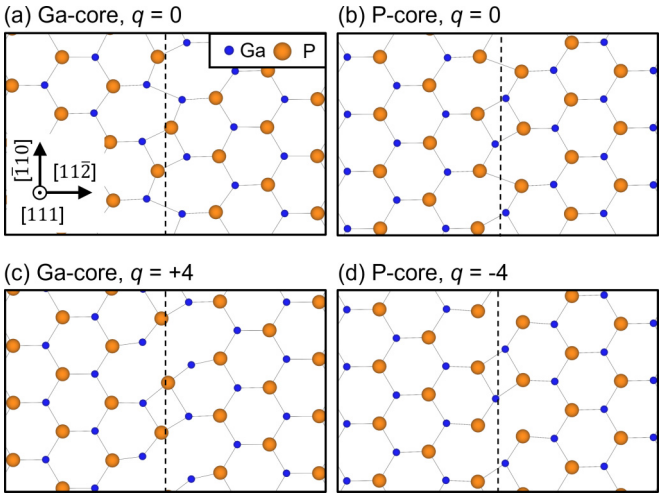

FIG. 9. Calculated intermediate structures of the Ga-core and P-core 30° partial dislocations in the neutral and charged states during glide. They are illustrated in the same manner as Fig. 1.

Figure 10 displays calculated Peierls potentials of the Ga-core dislocations. It can be seen that the Peierls-potential barrier height of the charged Ga core is much smaller than that of the neutral one. This proves that the charged Ga-core dislocation has less resistance to glide motion, as compared to the neutral one. Such a reduced potential barrier height for

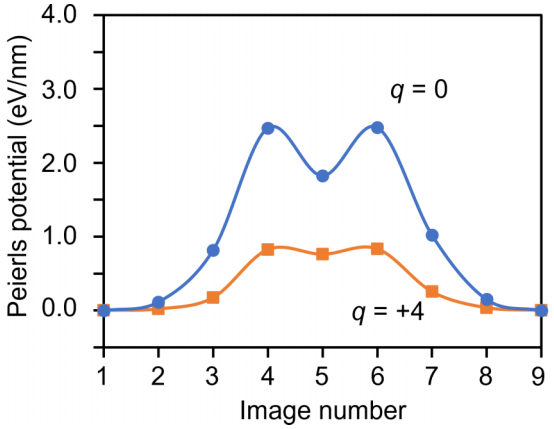

FIG. 10. Calculated Peierls potentials of the Ga-core 30° partial dislocations in the neutral and charged ($q = +4$) states by using NEB. The image numbers of 1 and 9 indicate the partial dislocations at the stationary positions on the slip plane, and the potential energy of the image 1 was set at zero. The image 5 corresponds to the central intermediate atomic structures shown in Fig. 9.

TABLE II. Calculated ΔE_P for the Ga and P cores with different charge states q.

	q	ΔE_P (eV/nm)
Ga core	0	1.77
	+4	0.74
	+3	0.74
	+2	0.74
P core	0	2.10
	–4	0.01
	–3	0.01
	–2	0.01

glide of the charged dislocation can be understood because of the unreconstructed structure. The neutral dislocation should break the additional Ga-Ga bonds at the core upon glide [Fig. 1(c)], whereas glide motion of the charged dislocation without such like-atom bonds [Fig. 1(a)] can be attained only by bond breaking and bond reformation between Ga and P.

Moreover, the potential of the neutral Ga-core dislocation has two explicit peaks at the images 4 and 6. This is mainly because the Ga-Ga bonds in the intermediate structure at the image 5 [see Fig. 9(a)] should also be broken during the glide. Since such like-atom bonds are not involved in the intermediate structure of the charged Ga core [Fig. 9(c)], the variation of the potential around the saddle point is not so significant.

As is well known, NEB calculations are computationally demanding. To qualitatively but systematically investigate how different the Peierls-potential barrier heights are in the different cores and different charged states, the potential-energy differences between the most stable structure and the intermediate structure were calculated and considered to be simplified potential barrier heights for dislocation glide (ΔE_P). This is reasonable from the results of the Ga core in Fig. 10 because the potential-energy difference at the central image 5 reflects the difference in Peierls-potential barrier height clearly.

As can be seen in Table II, ΔE_p values of the Ga and P cores in the absence of excess carriers ($q = 0$) were found to be about 2 eV/nm, while in the presence of excess holes and electrons, ΔE_P values of the Ga and P cores decreased by less than half and were almost independent of the charge states. It can be said that the atomic-structure changes from reconstruction to unreconstruction due to carrier trapping can significantly reduce resistance to dislocation glide in GaP, which may in turn lead to increased dislocation mobility. This corresponds to the fact that partial dislocations in GaP have larger mobilities under light illumination, as found experimentally [5].

As a final note, a plausible key factor for the PPE is discussed. According to experimental reports and theoretical calculations for II-VI group semiconductors, the material systems exhibited the p-PPE, which can be well understood on the basis of the energetically most favorable atomic structures of partial-dislocation cores [15,16,18]. Partial dislocations in II-VI semiconductor crystals tend to have the unreconstructed atomic structures in the pristine state, whereas they are transformed to the reconstructed atomic structures in the presence of excess carriers. Since the reconstructed atomic structures should be broken repeatedly during glide, the formation of such reconstructed cores can become obstacles for dislocation glide under light illumination. In contrast, III-V and IV-IV group semiconductor crystals like GaAs as well as GaP were experimentally reported to show the n-PPE. Partial dislocations in these systems were found to have the reconstructed atomic structures without any carriers [38,41,50]. As argued in the present study, however, the dislocation cores are transformed into the unreconstructed states in the presence of excess carriers. It can be said, therefore, that a major difference between the above two systems is the dislocation-core structures in the pristine state (without excess carriers). The importance of dangling bonds at the dislocation cores in III-V and IV-IV semiconductor crystals indicates that ionicity or covalency of the host crystals should be one of the essential factors to determine either the n-PPE or the p-PPE. We would like to suggest that the PPE of the inorganic compound semiconductors can be comprehensively explained in terms of atomic-structure change at the partial dislocation cores.

V. CONCLUSIONS

The core structures of 30° Shockley partial dislocations in GaP with and without excess carriers were investigated by GGA+U calculations. In the absence of excess carriers, the lowest-energy atomic structures of the Ga-core and P-core partial dislocations were found to be reconstructed. In the presence of excess carriers, the reconstructed Ga and P cores trapped excess holes and electrons, respectively, and they were subsequently transformed into the unreconstructed structures. From an evaluation of energy barrier heights for dislocation glide, it was found that the Ga-core and P-core partial dislocations can have much smaller barrier heights for glide in the presence of excess carriers. This may correspond to the experimentally observed increased dislocation mobility in GaP under external light illumination.

ACKNOWLEDGMENTS

This work was supported by JSPS KAKENHI (Grants No. JP19H05786, No. JP22H04508, No. JP23KJ1059, and No. JP24H00379), JST-CREST (Grant No. JPMJCR17J1), JST FOREST Program (Grant No. JPMJFR223G, Japan), and a research grant from Kyosyo Hatta Foundation.

[1] H. Amano, Y. Baines, E. Beam, M. Borga, T. Bouchet, R. Chu, C. De Santi, and M. M. De Souza, The 2018 GaN power electronics roadmap, J. Phys. D **51**, 163001 (2018).

[2] S. Wang and P. Pirouz, Mechanical properties of undoped GaAs. Part I: Yield stress measurements, Acta Mater. **55**, 5500 (2007).

[3] B. E. Mdivanyan and M. S. Shikhsaidov, Photostimulated enhancement of dislocation glide in gallium arsenide crystals, Phys. Status Solidi **107**, 131 (1988).

[4] S. Koubaiti, J. J. Couderc, C. Levade, and G. Vanderschaeve, Photoplastic effect and vickers microhardness in III-V and II-VI semiconductor compounds, Mater. Sci. Eng. A **234–236**, 865 (1997).

[5] K. Maeda, O. Ueda, Y. Murayama, and K. Sakamoto, Mechanical properties and photomechanical effect in GaP single crystals, J. Phys. Chem. Solids **38**, 1173 (1977).

[6] L. Carlsson and C. Svensson, Photoplastic effect in ZnO, J. Appl. Phys. **41**, 1652 (1970).

[7] C. N. Ahlquist, M. J. Carroll, and P. Stroempl, The Photoplastic effect in wurtzite and sphalerite structure II-VI compounds, J. Phys. Chem. Solids **33**, 337 (1972).

[8] Y. A. Osip'yan, V. F. Petrenko, A. V. Zaretskii, and R. W. Whitworth, Properties of II–VI semiconductors associated with moving dislocations, Adv. Phys. **35**, 115 (1986).

[9] Y. Oshima, A. Nakamura, and K. Matsunaga, Extraordinary plasticity of an inorganic semiconductor in darkness, Science **360**, 772 (2018).

[10] K. Matsunaga, M. Yoshiya, N. Shibata, H. Ohta, and T. Mizoguchi, Ceramic science of crystal defect cores, J. Ceram. Soc. Jpn. **130**, 648 (2022).

[11] A. Nakamura, X. Fang, A. Matsubara, E. Tochigi, Y. Oshima, T. Saito, T. Yokoi, Y. Ikuhara, and K. Matsunaga, Photoindentation: A new route to understanding dislocation behavior in light, Nano Lett. **21**, 1962 (2021).

[12] H. Oguri, Y. Li, E. Tochigi, X. Fang, K. Tanigaki, Y. Ogura, K. Matsunaga, and A. Nakamura, Bringing the photoplastic effect in ZnO to Light: A photoindentation study on pyramidal slip, J. Eur. Ceram. Soc. **44**, 1301 (2024).

[13] Y. Li, H. Oguri, A. Matsubara, E. Tochigi, X. Fang, Y. Ogura, K. Matsunaga, and A. Nakamura, Strain-rate insensitive photoindentation pop-in behavior in ZnS single crystals at room temperature, J. Ceram. Soc. Jpn. **131**, 23064 (2023).

[14] Y. Li, Shedding new light on the dislocation-mediated plasticity in wurtzite ZnO single crystals by photoindentation, J. Mater. Sci. Technol. **156**, 206 (2023).

[15] K. Matsunaga, S. Hoshino, M. Ukita, Y. Oshima, T. Yokoi, and A. Nakamura, Carrier-trapping induced reconstruction of partial-dislocation cores responsible for light-illumination controlled plasticity in an inorganic semiconductor, Acta Mater. **195**, 645 (2020).

[16] S. Hoshino, Y. Oshima, T. Yokoi, A. Nakamura, and K. Matsunaga, DFT calculations of carrier-trapping effects on atomic structures of 30° partial dislocation cores in zincblende II-VI group zinc compounds, Phys. Rev. Mater. **7**, 013603 (2023).

[17] B. Feng, S. Hoshino, B. Miao, J. Wei, Y. Ogura, A. Nakamura, E. Tochigi, K. Matsunaga, Y. Ikuhara, and N. Shibata, Direct observation of intrinsic core structure of a partial dislocation in ZnS, J. Ceram. Soc. Japan **131**, 659 (2023).

[18] S. Hoshino, T. Yokoi, Y. Ogura, and K. Matsunaga, Electronic and atomic structures of shockley-partial dislocations in CdX (X = S, Se and Te), J. Ceram. Soc. Jpn. **131**, 23055 (2023).

[19] Y. Oshima, A. Nakamura, K. P. D. Lagerlöf, T. Yokoi, and K. Matsunaga, Room-temperature creep deformation of cubic ZnS crystals under controlled light conditions, Acta Mater. **195**, 690 (2020).

[20] J. D. Weeks, J. C. Tully, and L. C. Kimerling, Theory of defect reactions in semiconductors, Phys. Rev. B **12**, 3286 (1975).

[21] H. Sumi, Dynamic defect reactions induced by multiphonon nonradiative recombination of injected carriers at deep levels in semiconductors, Phys. Rev. B **29**, 4616 (1984).

[22] K. Maeda and S. Takeuchi, *Dislocations in Solids* (Elsevier, New York, 1996), Vol. 10.

[23] P. E. Blöchl, Projector augmented-wave method, Phys. Rev. B **50**, 17953 (1994).

[24] G. Kresse and J. Hafner, *Ab Initio* molecular dynamics for open-shell transition metals, Phys. Rev. B **48**, 13115 (1993).

[25] J. P. Perdew, K. Burke, and M. Ernzerhof, Generalized gradient approximation made simple, Phys. Rev. Lett. **77**, 3865 (1996).

[26] C. Freysoldt, B. Grabowski, T. Hickel, J. Neugebauer, G. Kresse, A. Janotti, and C. G. Van de Walle, First-principles calculations for point defects in solids, Rev. Mod. Phys. **86**, 253 (2014).

[27] F. Oba, M. Choi, A. Togo, and I. Tanaka, Point defects in ZnO: An approach from first principles, Sci. Technol. Adv. Mater. **12**, 034302 (2011).

[28] S. L. Dudarev, G. A. Botton, S. Y. Savrasov, C. J. Humphreys, and A. P. Sutton, Electron-energy-loss spectra and the structural stability of nickel oxide: An LSDA+U study, Phys. Rev. B **57**, 1505 (1998).

[29] P. Khatri and M. N. Huda, Application of attractive potential by DFT + U to predict the electronic properties of materials without highly localized bands, Comput. Mater. Sci. **81**, 290 (2014).

[30] See Supplemental Material at http://link.aps.org/supplemental/10.1103/PhysRevMaterials.8.093605 for the comparison of formation energies between GGA+U and GGA and the atomic structures of the charged partial dislocation with reconstructed Ga core and unreconstructed P core.

[31] J. Heyd, G. E. Scuseria, and M. Ernzerhof, Hybrid functionals based on a screened Coulomb potential, J. Chem. Phys. **118**, 8207 (2003).

[32] Y. Hinuma, A. Grüneis, G. Kresse, and F. Oba, Band alignment of semiconductors from density-functional theory and many-body perturbation theory, Phys. Rev. B **90**, 155405 (2014).

[33] P. L. Gai and A. Howie, Dissociation of dislocations in GaP, Philos. Mag. **30**, 939 (1974).

[34] D. Rodney, L. Ventelon, E. Clouet, L. Pizzagalli, and F. Willaime, *Ab Initio* modeling of dislocation core properties in metals and semiconductors, Acta Mater. **124**, 633 (2017).

[35] J. Bennetto, R. W. Nunes, and D. Vanderbilt, Period-doubled structure for the 90° partial dislocation in silicon, Phys. Rev. Lett. **79**, 245 (1997).

[36] R. W. Nunes, J. Bennetto, and D. Vanderbilt, Core reconstruction of the partial dislocation in nonpolar semiconductors, Phys. Rev. B **58**, 12563 (1998).

[37] R. W. Nunes, J. Bennetto, and D. Vanderbilt, Atomic structure of dislocation kinks in silicon, Phys. Rev. B **57**, 10388 (1998).

[38] J. F. Justo, V. V. Bulatov, and S. Yip, Dislocation core reconstruction and its effect on dislocation mobility in silicon, J. Appl. Phys. **86**, 4249 (1999).

[39] G. Savini, M. I. Heggie, and S. Öberg, Core structures and kink migrations of partial dislocations in 4H-SiC, Farad. Discuss. **134**, 353 (2007).

[40] G. Savini, A. T. Blumenau, M. I. Heggie, and S. Öberg, Structure and energy of partial dislocations in wurtzite-GaN, Phys. Status Solidi **4**, 2945 (2007).

[41] J. S. Park, B. Huang, S. H. Wei, J. Kang, and W. E. McMahon, Period-doubling reconstructions of semiconductor partial dislocations, NPG Asia Mater. **7**, e216 (2015).

[42] K. E. Kweon, D. Åberg, and V. Lordi, First-principles study of atomic and electronic structures of 60° perfect and 30°/90° partial glide dislocations in CdTe, Phys. Rev. B **93**, 174109 (2016).

[43] C. Freysoldt, J. Neugebauer, A. M. Z. Tan, and R. G. Henning, Limitations of empirical supercell extrapolation for calculations of point defects in bulk, at surfaces, and in two-dimensional materials, Phys. Rev. B **105**, 014103 (2022).

[44] P. M. Anderson, J. P. Hirth, and J. Lothe, *Theory of dislocations*, 3rd ed. (Cambridge University Press, New York, 2017).

[45] M. Ukita, A. Nakamura, T. Yokoi, and K. Matsunaga, Electronic and atomic structures of edge and screw dislocations in rock salt structured ionic crystals, Philos. Mag. **98**, 2189 (2018).

[46] T. Suzuki and S. Takeuchi, Deformation of crystals controlled by the peierls mechanism of the smooth kink regime, in *Crystal Lattice Defects and Dislocation Dynamics,* edited by R. A. Vardanian, (Nova Science, New York, 2001).

[47] H. Koizumi, H. O. K. Kirchner, and T. Suzuki, Kink pair nucleation and critical shear stress, Acta Metall. Mater. **41**, 3483 (1993).

[48] G. Henkelman, B. P. Uberuaga, and H. Jonsson, A climbing image nudged elastic band method for finding saddle points and minimum energy paths, J. Chem. Phys. **113**, 9901 (2000).

[49] L. Huang and S. Wang, A theoretical investigation of the glide dislocations in the sphalerite ZnS, J. Appl. Phys. **124**, 175702 (2018).

[50] M. M. De Araújo, J. F. Justo, and R. W. Nunes, Electronic charge effects on dislocation cores in silicon, Appl. Phys. Lett. **85**, 5610 (2004).